

Dynamic State Warping

Zhichen Gong and Huanhuan Chen, *Senior Member, IEEE*

Abstract—The ubiquity of sequences in many domains enhances significant recent interest in sequence learning, for which a basic problem is how to measure the distance between sequences. Dynamic time warping (DTW) aligns two sequences by nonlinear local warping and returns a distance value. DTW shows superior ability in many applications, e.g. video, image, etc. However, in DTW, two points are paired essentially based on point-to-point Euclidean distance (ED) without considering the autocorrelation of sequences. Thus, points with different semantic meanings, e.g. peaks and valleys, may be matched providing their coordinate values are similar. As a result, DTW is sensitive to noise and poorly interpretable. This paper proposes an efficient and flexible sequence alignment algorithm, dynamic state warping (DSW). DSW converts each time point into a latent state, which endows point-wise autocorrelation information. Alignment is performed by using the state sequences. Thus DSW is able to yield alignment that is semantically more interpretable than that of DTW. Using one nearest neighbor classifier, DSW shows significant improvement on classification accuracy in comparison to ED (70/85 wins) and DTW (74/85 wins). We also empirically demonstrate that DSW is more robust and scales better to long sequences than ED and DTW.

Index Terms—Recurrent neural network, Representation learning, Time series classification.

1 INTRODUCTION

SEQUENCES are generated and analyzed in almost every domain of human society such as medical [1], engineering [2], entertainment [3], etc. Computing the distance between sequences is critical for classification and has attracted significant research interest [4], [5], [6].

For sequence classification, one nearest neighbor (1NN) classifier has been empirically shown to be a strong solution with proper distance measurements [7], [8], [9]. 1NN classifier is intrinsically parameter-free. In this case, the only concern is how to measure the distance between sequences properly [10].

Note that sequences are different from typical vectorial data. Sequences are high dimensional, auto-correlated among temporal axes and possibly of varying length. Therefore, to measure the distance between sequences, consideration has to be given to the properties of sequences, such as nonlinear local warping, phase shift and scaling distortion etc. A more comprehensive review can be found in [10].

Dynamic time warping (DTW) [11], [12] is to compute the distance between two sequences by warping them locally to the same length. It allows one-to-many mappings between sequences to “stretch” a sequence or many-to-one mappings to “condense” a sequence. In this way, DTW is naturally compatible with phase distortion invariance of sequential data [10]. Despite the simplicity of DTW, 1NN classifier with DTW distance has been very successful in many applications, such as video, image and audio etc. [9], [13], [14]. It has been a consensus that DTW may be the strongest distance measurements for sequences [15], [16].

DTW aligns two sequences by taking the point-to-point comparison of coordinate values as a fundamental unit [16]. Concretely, one point on a sequence is compared to all or a subset of points on the other sequence to compute a point level distance. In doing so, one can find an alignment path

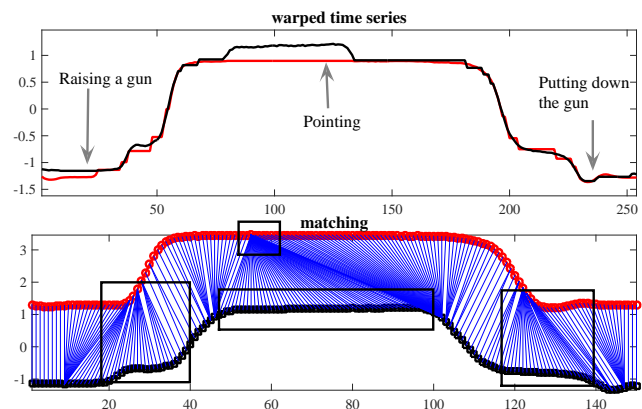


Fig. 1. DTW alignment of GunPoint dataset. The sequences presents three stages clearly, i.e. raising a gun, pointing and putting down the gun. DTW is unable to find the discriminative features between two sequences ([20~40] and [120~140]). We also observe a severe distortion that DTW matches one point on the upside sequence to almost the whole subsequence of the downside sequence.

such that the aligned sequences yields a globally minimum Euclidean distance [11], which is returned as the distance between the original sequences. However, this point-level comparison usually cannot provide dynamic evidence for matching two points. Note that from human’s intuition, we intend to pair two points of two sequences by taking into account the nearby points or even the global structure. Thus, DTW does align globally but is unable to take into consideration the auto-correlated structure information properly [8]. This makes DTW fragile to noise [12], which is also demonstrated in our experiment (Section 4). As pointed out in [8], [17], DTW usually has weak interpretability of its alignment. Concretely, the alignment result may lack local semantic meanings. For example, DTW may match points on a local peak and a valley if their Euclidean distance is small. Besides, DTW may match one point to too many points resulting in un-intuitive alignment results and de-

• Z. Gong and H. Chen are with UBRI, School of Computer Science and Technology, University of Science and Technology of China, Hefei 230027, China (e-mail: zcgong@mail.ustc.edu.cn; hchen@ustc.edu.cn;

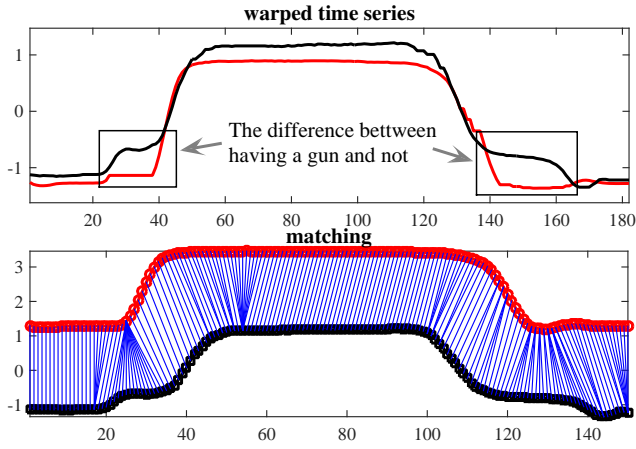


Fig. 2. DSW alignment of GunPoint dataset. The alignment of DSW is semantically more sensible than that of DTW. The discriminative features, i.e. having a gun or not, is detected.

grade the classification performance [2].

Figure 1 illustrates the DTW match result of GunPoint dataset from UCR time series archive [18]. The two sequences are from two different classes. Briefly speaking, GunPoint dataset contains two class of motion track sequences of an actress. Each motion includes three processes: raising a gun, pointing and putting down the gun. For the first class, the gun is initially in a hip-mounted holster. For the second class, the gun is initially in the hand of the actress instead of the holster. In time points roughly ranging in [20~40] and [120~140], the two sequences differ slightly by whether the actress takes a gun or not. According to Figure 1, DTW fails to capture this difference, and it returns nearly “perfect” alignment for two semantically different sequences. Besides, it is shown that DTW un-intuitively maps one point to many points on the other sequence.

Time points of a sequence have dependencies over time axis, which provides latent regime characterizing the sequence behavior. DTW is unable to take into consideration this information. To mitigate the problem with DTW and motivated by the advance of representation learning, in this paper, we propose a novel sequence alignment algorithm, dynamic state warping (DSW). DSW efficiently converts time points on a sequence into the corresponding hidden states, which has integrated characteristics of the past history and the current point. In this way, the state evolving sequence may be “aware” of the sequential order information and encodes the generating mechanism of original sequences. Dynamic programming technique is employed to align the state sequences instead of the temporal points. Therefore, DSW is prone to match time points with similar states together.

The time complexity of the state converting process for two given sequences of length L_Q and L_C is $O(L_Q + L_C)$. The alignment process takes time complexity $O(L_Q L_C)$. Then the overall cost is $O(L_Q L_C)$, at the same level as that of DTW.

Our method has several advantages: (1) DSW explicitly takes advantages of the autocorrelation structure characteristics of sequential data. It provides versatile and flexible discriminative state representations for sequences; (2) The

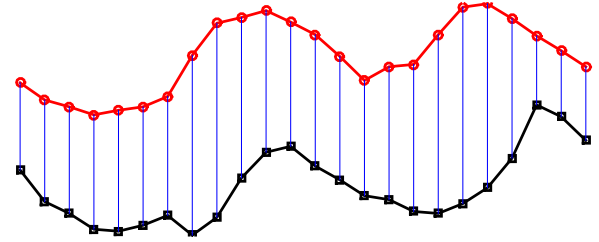


Fig. 3. Illustration of Euclidean distance.

alignment results of DSW is semantically more interpretable than plain DTW; (3) Using one nearest neighbor classifier, DSW exhibits lower error rates than DTW on most datasets; (4) The flexibility of DSW allows users to fine tune the representations of sequences to capture the discriminative features for specific tasks; (5) DSW is able to deal with univariate and multivariate sequences without adjusting the algorithm. (6) DSW shows more robustness to noise and more suitable for long sequences than compared methods; (7) After obtaining the state sequences, the problem is again DTW, thus advanced techniques [9], [19] for improving the effectiveness and efficiency of DTW is also compatible with DSW.

As a comparison, Figure 2 demonstrates the alignment result of DSW on GunPoint dataset. The parameters of DSW are determined randomly. First of all, it is noticeable that DSW is able to match two sequences correctly and consistently with the three true actions. Second, whether the actress takes a gun out of the holster or holding a gun in hand, is distinguished correctly.

Our contributions in this work include: (1) We propose a novel state alignment algorithm for sequences. This algorithm is as efficient as DTW but provides more interpretable and accurate alignments. (2) By combining with one nearest neighbor classifier, our method achieves significantly better classification results than DTW. (3) We perform extensive experiments comparing our method with Euclidean distance (ED) and DTW. We also empirically analyze the relating properties of the state converting component of DSW extensively. (4) Our strategy provides a general learning framework and it is possible to incorporate discriminative learning and representation learning techniques.

The rest of this paper is organized as follows: in Section 2, we introduce preliminary knowledge about time series classification, DTW and recurrent neural networks; in Section 3, we introduce DSW in detail; Section 4 performs extensive experiments to evaluate DSW; finally, Section 5 concludes this paper.

2 BACKGROUND AND RELATED WORK

In this section, we first clarify some notations and basic knowledge about sequence learning. Then we introduce the DTW algorithm in detail. Since our method is based on recurrent neural networks, we introduce recurrent neural networks at last.

2.1 Sequence Distance

A sequence is a series of observations for at least one variable. We use a matrix $X = [x^1, x^2, \dots, x^{L_x}]^T \in R^{L_x \times d}$

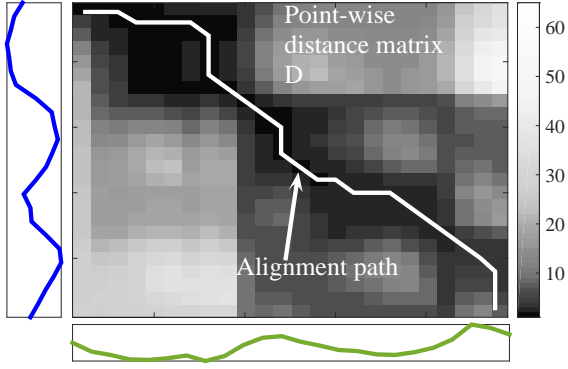


Fig. 4. Illustration of searching for the optimal alignment using DTW. The two sequences are demonstrated on the left and bottom. The point-wise distance matrix and the optimal alignment path are presented.

to denote a sequence, where $x^i \in R^{d \times 1}$ ($i \in [1, L_X]$) is an observation at a time point indexed by i , L_X is the length of series X and d is the number of variables. Each sequence is associated with a label y . The task of classification is to learn a function mapping from X to y .

Given two sequences Q and C , if they are of equal length, one can easily compute their distance using Euclidean distance (ED) or p-norm distance [20], such as $ED(Q, C) = \sqrt{\sum_{i=1}^L \sum_{j=1}^d ((q^{i,j} - c^{i,j})^2)}$. This kind of distance is also called lock-step distance since it matches elements of sequences according to their position (See Figure 3).

However, in most real-world applications, sequences may be of varying length. In this case, elastic distance, such as DTW and longest common subsequence [15] etc., is used to compute the distance.

2.1.1 Dynamic Time Warping

Given two sequences Q and C of possibly different lengths, DTW stretches or condenses two sequences to the same length. DTW allows nonlinear local warping to take into account possible distortions. It finds an optimal alignment between Q and C such that the accumulative Euclidean distance is minimized [12]. In doing so, it returns a distance value that measures the similarity between the two sequences.

Denote $D \in R^{L_Q \times L_C}$ as the distance matrix of time points of Q and C . DTW algorithm travels from the position $[1, 1]$ to position $[L_Q, L_C]$ of D to find a sequence of indices A and B of the same length $l \geq \max\{L_Q, L_C\}$ such that the cumulative distance $\sum_{i=1}^l D_{A_i, B_i}$ is minimized. In this way, the point $A(i)$ of sequence Q is matched with the point $B(i)$ of sequence C . See Figure 4 for an illustration.

To be a valid alignment, the paths A and B have to satisfy three constraints:

- 1) $A(1) = 1, B(1) = 1$
- 2) $A(l) = L_Q, B(l) = L_C$
- 3) $\forall i \in [1, l-1], (A(i+1), B(i+1)) - (A(i), B(i)) = \{(0, 1), (1, 0), (1, 1)\}$

Hence, the alignment of two sequences should start from the first time point and end with the last point. Each time

point has at least one matching point on the other sequence. The match increases monotonically.

Formally, denote $\alpha \in \{0, 1\}^{l \times L_Q}$ and $\beta \in \{0, 1\}^{l \times L_C}$ be two warping matrices corresponding to the warping path A and B . Let $\alpha(i, A(i)) = 1, \beta(i, B(i)) = 1$, where $i \in \{1, 2, \dots, l\}$. All other entries are zero. In this case the two warped sequences become $\alpha \times Q$ and $\beta \times C$. The overall cost function of DTW is generalized as:

$$\begin{aligned} Cost &= \arg \min_{l, A, B} \left(\sum_{i=1}^l D_{A_i, B_i} \right) \\ &= \arg \min_{l, \alpha, \beta} (\alpha \times Q - \beta \times C)^2 \end{aligned} \quad (1)$$

Therefore, DTW is essentially Euclidean distance except that local distortion is allowed. The above cost function can be solved with time complexity $O(L_Q L_C)$ using dynamic programming:

$$Cost(m, n) = D(m, n) + \min \left\{ \begin{array}{l} D(m-1, n), \\ D(m-1, n-1), \\ D(m, n-1) \end{array} \right\}$$

2.1.2 Related Work

Numerous trials have been made to enhance DTW, which can be roughly divided into two categories: adjusting the point-wise distance (e.g. [12], [13], [21]) and heuristically constraining the DTW (e.g. [10], [19]).

Garreau et al. [21] proposed to learn a distance metric for measuring the similarity between two points. However, this method takes the difference between the empirical alignment and true alignment as the cost function. Therefore, it requires the true alignments among sequences, which is not available for many real-world applications. Besides, it is only feasible for multi-variate sequence alignment. Zhou et al. [13] combined DTW with canonical correlation analysis (CCA), termed canonical time warping (CTA). The point-wise distance is linearly transformed by CCA. CTA alternatively optimizes the CCA and DTW alignment to minimize the accumulative distance. However, CTA is only applicable for multivariate sequences. The objective function of CTW is non-convex and may return local minima.

In [22], Petitjean et al. proposed to replace multiple sequences with an average sequence $\hat{T} = \arg \min_{\hat{T}} \{DTW(T_i, \hat{T})\}_{i=1}^N$ using the DTW distance. But it does not have a contribution on improving the alignment of DTW algorithm. Keogh and Pazzani [12] proposed to replace the coordinator distances by the derivative distance (DDTW). Therefore, points with similar changing trend are matched. Jeong et al. [19] proposed to weight the match of two points by the length of stretch such that the long shift is penalized (WDTW). A combination of WDTW and DDTW is also considered (WDDTW). Batista et al. [10] proposed a similar penalty-based distance. That method additionally considers a coefficient on top of the DTW distance in order to avoid small distance between sequences of different complexity (CID-DTW). Like DTW, DDTW, WDTW and CID-DTW still have the limitation in considering the sequential nature of data. Other studies focus on improving the efficiency of DTW [9] but do not improve the alignment results of DTW.

Our method DSW is similar to methods adjusting the point-wise distance. But DSW is different from previous methods in that DSW is able to utilize the sequential dynamic information of sequences. From Equation (1), it is clear that given the distance matrix D , the basic subroutine of DTW is the point-wise Euclidean distance of temporal axis coordinate values. The point-to-point distance ignores local autocorrelation structure information. This is the key bottle-neck of the classification performance of DTW. In this paper, we are going to offer a remedy by taking advantage of the memory ability of recurrent networks to learn a state representation for each time point. The alignment is performed in the state space of sequences instead of the time domain.

2.2 Recurrent Neural Network and Reservoir Computing

Recurrent neural network (RNN) enables recurrent connections among neurons. RNN learns a representation for each time point that takes into account the previous input history and the current input. Unlike HMM, which ignored earlier points beyond a threshold, RNNs do not constrain the memory length [23]. In RNN, the far earlier inputs give less influence to the representation of the current input. This implicit fading memory has enabled RNN a powerful tool in language modeling [24], sequence process [4] and video prediction [3] etc.

Reservoir network is a type of RNN. It has a high dimensional recurrent network that is fixed during training called reservoir. The reservoir provides general dynamical features for input sequences providing it is designed properly. In [2], the output weights of the reservoir model is proved to be able to extract discriminative features from the whole sequence. It assumes that the generating mechanism of the sequences is time-invariant. Similarly, Fisher kernel [25] learns vectorial fisher score as a representations for the whole sequence using a probabilistic generative model. Fisher kernel assumes that similar objects stretch the generative model parameters to a similar extent. In Fisher kernel, all the sequences have to be approximated by only one generative model, which seems to be restrictive.

This current work is different from previous studies. Our goal is to uncover the state transition track by learning state space representations for time points, rather than a representation of the whole sequence. Thus the assumption of the time-invariant generating mechanism is not a limitation for DSW. Besides, it is critical for model space learning method to learn faithful models for original sequences. So a large reservoir is usually needed, which adds computational burdens. For more information about RNN and reservoir, we refer the readers to [26].

DTW is commonly used comparing time points in the time domain in previous sequence classification methods, which makes it sensitive to noise and weakly interpretable [8]. Numerous methods have been proposed to improve the effectiveness or efficiency of DTW. However, little prior work has contributed from the aspect of learning point-wise representations to enhance DTW for sequence classification.

As a remedy, in this work, we propose to learn temporal point representations for sequences. We learn flexible and

versatile representations for each time point. The integrated information in the time point representations provides discriminative features. The proposed method makes use of the history information of sequences to make the alignment semantically more sensible and provides better classification accuracy in comparison with DTW.

3 DYNAMIC STATE WARPING

This section introduces the dynamic state warping method. Sequences are structured objects that have correlation among different time points. DTW finds an optimal alignment between two sequences so that the cumulative Euclidean distance is minimized. However, it has limitations in making use of the dynamic information.

We propose an algorithm DSW as a mitigation. In particular, the mechanism of DSW is a two-stage process. In the first stage, DSW uses the reservoir network as a general purpose temporal filter to convert original sequences into state sequences, which encapsulates the generating mechanism of original sequences. In the second stage, the same alignment operation as that of DTW is performed to align the state trajectory sequences.

The motivations of choosing the reservoir network as the signal-to-state converting model include: (1) it provides parsimonious state representations for sequences points efficiently; (2) it is able to take advantage of the sequential autocorrelation information of sequences; (3) it requires much less effort to tune the network compared with a classical neural network.

Echo state network (ESN) is a kind of reservoir model. ESN is characterized by a non-trainable high dimensional nonlinear dynamical reservoir and an efficiently trained linear readout layer. The reservoir is randomly generated under the constraint of the maximum eigenvalue being less than one. This is also called echo state property. Loosely speaking, it requires that the initial inputs have little influence on the final state. It is usually implemented by first normalizing the reservoir weight matrix to have unitary spectral radius. Then we multiply it with a scaling parameter. The readout layer assembles the state space features of the reservoir to learn a function mapping from reservoir state to the output sequence. Linear regression is usually employed to learn the functions.

In this study, we are not going to count on the assembling ability of the readout layer, but we will analyze its effect on the performance of DSW in the experiment (See Section 4.6.3). The approximation ability of the ESN reservoir helps leverage the autocorrelation of original sequences.

To justify the randomness of ESN, Rodan et al. [27] propose a topologically fixed reservoir, cycle reservoir with jumps (CRJ). CRJ reservoir is more constrained than ESN reservoir. It connects the reservoir neurons in a unidirectional circle and allows fixed length jumps on the circle. In this case, there are only three kind of connections for CRJ reservoir, i.e. input, jump and cyclic connections. The network weights can be determined by three values $r = \{r_i, r_j, r_c\}$ for each kind of connection.

This paper takes CRJ as the base model for ease of analysis. The DSW algorithm is demonstrated in Algorithm

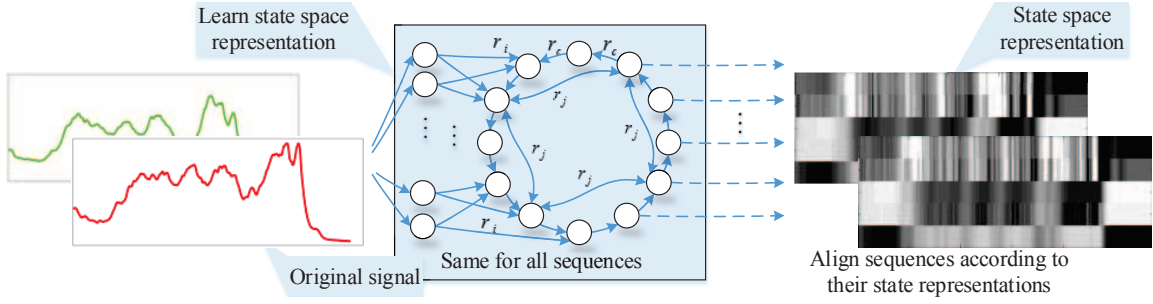


Fig. 5. The semantic demonstration of the key idea of DSW. The CRJ reservoir network converts the original sequences to state trajectory sequences. Then two points are paired if their states are similar.

1. Figure 5 gives a sematic illustration of the key idea of this paper.

Algorithm 1 Dynamic state warping

- 1: **Input:** Two sequences $Q \in R^{L_Q \times d}, C \in R^{L_C \times d}$; #neurons of the reservoir; jump length of reservoir; initial parameters for network ($\{r_i, r_c, r_j\}$).
 - 2: **Output:** A distance between the two sequences.
 - 3: Use the CRJ network to convert the original sequences into reservoir state space.
 - 4: Compute state point level distance matrix D .
 - 5: Search the optimal warped path α and β using dynamic programming.
 - 6: Return the accumulative distance (Equation (1)) as the distance between two input sequences.
-

The form of CRJ is generalized as:

$$\begin{cases} \mathbf{S}(t+1) = g(\mathbf{R}\mathbf{S}(t) + \mathbf{V}\mathbf{X}(t+1)) \\ f(t) = g_{out}(\mathbf{W}\mathbf{S}(t) + b) \end{cases} \quad (2)$$

where $S(t) \in R^N$ is the reservoir state, N is the number of neurons in the reservoir; $X(t) \in R^n$ is the input sequence, n is the number of input neurons; $\mathbf{R} \in R^{N \times N}$ is the reservoir weight matrix, $\mathbf{V} \in R^{N \times n}$ is the input weight matrix, $\mathbf{W} \in R^{O \times N}$ is the output weight matrix, $b \in R^O$ is the bias term, O is the number of output neurons; g is the state transition function, which is a nonlinear function and usually taken as \tanh or the sigmoid function. g_{out} is the activation function of outputs. Without loss of generality, in this paper, we fix $g = \tanh$ and g_{out} as identity function.

Given an input sequence $X \in R^{L \times d}$, we first drive it through the nonlinear dynamic reservoir and obtain a state transition trajectory sequence $S \in [-1, 1]^{L \times N}$, where N is the size of reservoir. It transforms from the previous state to a new state in the state space given a new input time point. In this way, the temporal signal space sequence is converted into multi-variate state space sequences. The state trajectory sequence encapsulates the generating mechanism of the original sequence by taking into consideration the previous state and current input (Equation (2)). In particular, the reservoir state representation is the activation of reservoir neurons with different driving input sequences. The state space representations provide discriminative features with more versatility and flexibility than original sequences.

We then employ DTW to align the state trajectory sequences as usual. It prefers to align points on two sequences with similar states.

Therefore, the difference between DTW and DSW lies in that DTW uses distance between time points as a subroutine, while DSW uses the distance of the state space representations.

Since our concern in this paper is to learn point-level states as representations, our framework can be naturally generalized to time-variant and time-invariant, uni-variate and multi-variate series.

Proposition: The state sequence is able to scale the noise in the original sequence by a constant scaling.

Proof: The state sequence is able to reduce the noise in the original signal by constraining r_i^2 . Given an additive noise ε in the sequence X , the distance between the state sequences is then:

$$\begin{aligned} & \|S^\varepsilon(t) - S(t)\|^2 \\ &= \|g(\mathbf{R}\mathbf{S}(t) + \mathbf{V}(X(t) + \varepsilon)) - g(\mathbf{R}\mathbf{S}(t) + \mathbf{V}X(t))\|^2 \\ &\leq \|\mathbf{R}\mathbf{S}(t) + \mathbf{V}(X(t) + \varepsilon) - \mathbf{R}\mathbf{S}(t) - \mathbf{V}X(t)\|^2 \\ &= \|\mathbf{V}\varepsilon\|^2 \leq r_i^2 \|\varepsilon\|^2 \end{aligned}$$

where S^ε is the noisy state sequence. The above equation reveals that the noise in the state sequence is scaled by the input weight r_i^2 . The nonlinear state transition function g can be \tanh or sigmoid function. Note that their derivative is not larger than one, thus we have $\tanh(\delta) \leq \delta$. That is, the noise level is reduced in the state sequence by adjusting r_i (usually $r_i \leq 1$ in the typical ESN setting [26]).

4 EXPERIMENT

In this section, we perform extensive experiments to evaluate our method. Since all the recent enhancement for DTW also works in DSW, our strategy is to compare DSW with DTW and ED primarily. We also compare DSW with more advanced algorithms for classification performance. In particular, this section is divided into four parts. We first evaluate our method on synthetic datasets to show its effectiveness as a distance metric (subsection 4.2). Secondly, the robustness is evaluated on synthetic noisy data. The scalability of long series is tested by consistently increasing the length of sequences (subsection 4.3). Thirdly, we evaluate DSW by the classification results on 85 UCR time series datasets [18] in comparison with ED, DTW and other algorithms (subsection 4.4 and 4.5). Finally, we analyze the

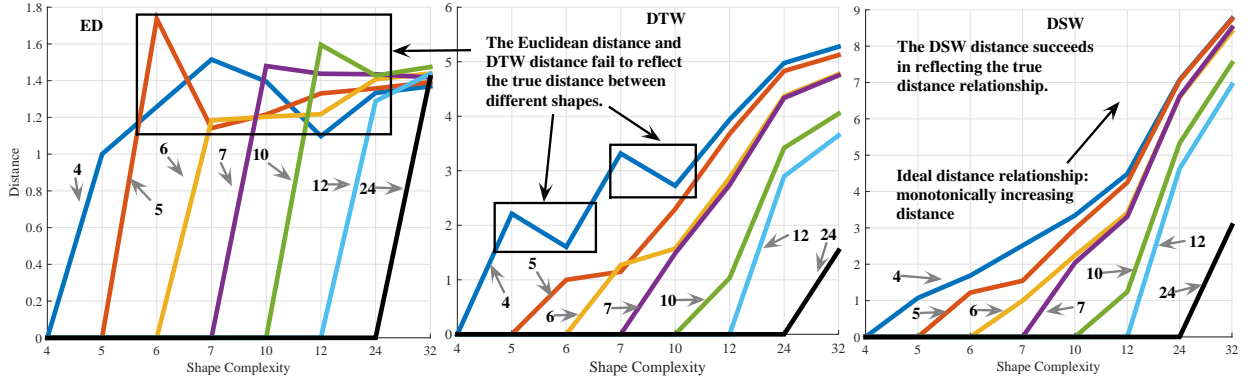


Fig. 6. Distance among shapes. The ylabel is the distance between the shapes. The xlabel indicates the shape labels. Each line indicates distance values of a shape to other shapes. Shapes with similar endpoints should share a small distance, while significantly different shapes share a large distance. It shows DSW approximate the true distance relationship well.

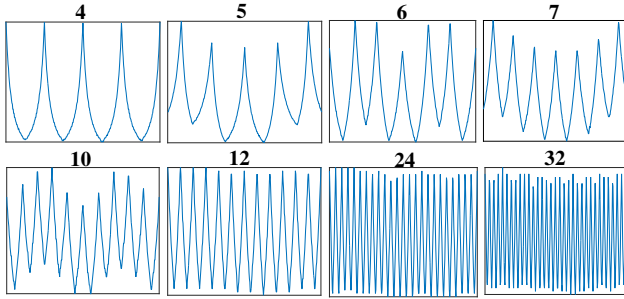


Fig. 7. Illustration of sequences of shapes with different number of endpoints.

relating properties of our method to provide more insights into DSW (subsection 4.6).

4.1 Experimental Setup

We compare DSW with Euclidean distance and DTW. For dynamic programming process, the size of warping window is not optimized. However, since the second stage of our method is intrinsically DTW, more advanced strengthening techniques for DTW, such as those proposed in [9] and [19], can be easily incorporated. Without explicit mention, the reservoir of DSW is randomly generated. The sequences have been normalized to have zero mean and unit standard deviation.

4.2 Distance Measurement

To demonstrate that DSW is a distance measurement that can approximate the true similarity structure of sequences, we compare DSW with Euclidean distance and DTW on a synthetic data. In particular, we consider the shapes of polygons [10], see Figure 8 for an illustration. The number of endpoints of a shape is taken as the label. For each polygon the original shape in two dimensional space is converted into one dimension series by computing the distance from the center to edge points. The resulting series is demonstrated in Figure 7.

Figure 6 demonstrates the distance among different shapes using Euclidean distance, DTW and DSW respectively. According to Figure 6, compared with ED and DTW,

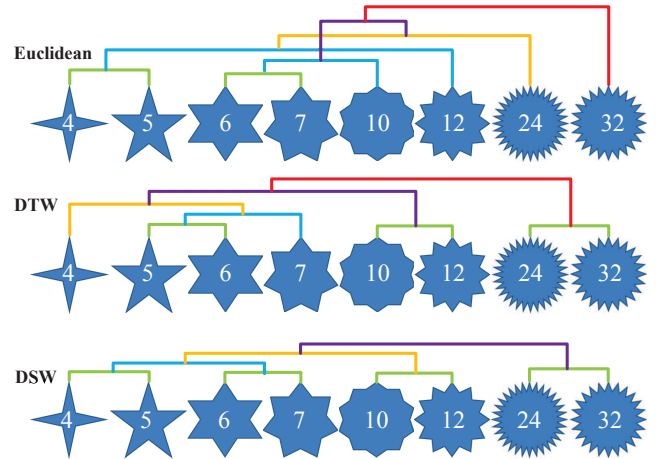


Fig. 8. Clustering results of shape sequences using Euclidean distance, DTW and DSW. DSW clusters shape sequences in a manner consistent with human's intuition. This result indicates that DSW is indeed effective in capturing the true similarity structure among sequences.

DSW captures the similarity between different shapes. Ideally, the distance between two shapes should increase with the difference of their complexity. Euclidean distance cannot approximate the true similarity relationship between polygons. DTW is better than Euclidean distance but fails in capturing the similarity between shape 4 and other shapes.

We also show the hierarchical clustering results of three distance measurements. As illustrated in Figure 8, DSW generates clustering result that is more consistent with the semantic meaning.

4.3 Robustness and Scalability

4.3.1 Robustness

To evaluate the robustness of different distance measurements, we conduct experiments varying the noise in the dataset. In detail, we choose a benchmark dataset Coffee [18]. On this dataset, the DTW and Euclidean distance achieve zero error rate when no additional noise is incorporated. We add a Gaussian white noise into coffee dataset with zero mean and standard deviation varying in the set $\{0.1, 0.3, 0.5, 0.7, 0.9, 1.1\}$. The standard deviation is set in this manner in order to clearly present the tendency. On each

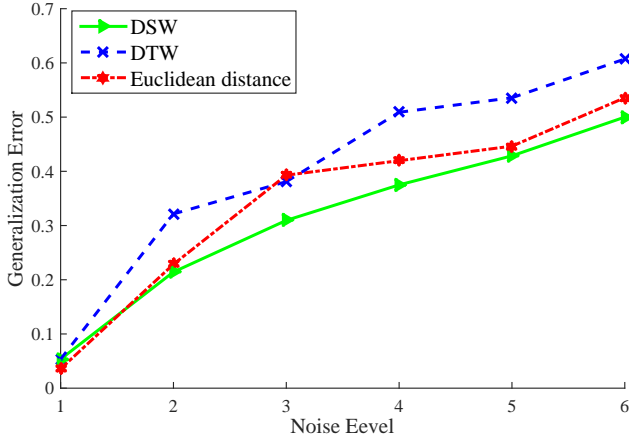


Fig. 9. The Generalization performance of Euclidean, DTW and DSW distance with 1NN classifier when facing noisy data. This result demonstrates that DSW is more robust than Euclidean distance and DTW.

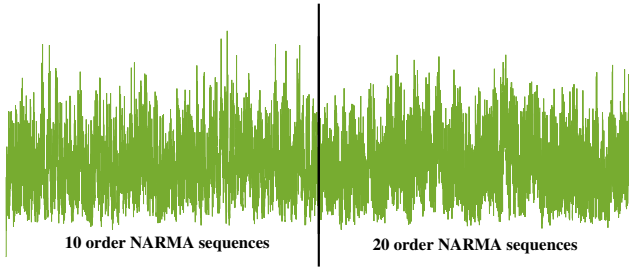


Fig. 10. Illustration of 10 order and 20 order NARMA synthetic sequences.

noise level, we perform 10 runs and report the average. The generalization error rate is computed using 1NN classifier with different distance measurement.

The results are presented in Figure 9. It shows that DSW is more robust to noise than competitive methods. DSW consistently achieves smaller generalization error rates than DTW, except that they are equal when noise level is 0.1. DTW is sensitive to noise because its basic unit is to compute point-wise Euclidean distance between points and counts heavily on the sequence shape during alignment. Yet, the Gaussian noise changes the magnitude of original sequences. This partially explains the noise sensitivity of DTW. Euclidean distance maintains intermediate performance. We also observe that when the noise level is low, Euclidean distance performs a little better than DTW and DSW distance.

4.3.2 Scalability to Long Sequences

In this subsection, we employ synthetic datasets containing varying length sequences to evaluate the scalability of DSW.

In particular, we generate a series of 10 order and 20

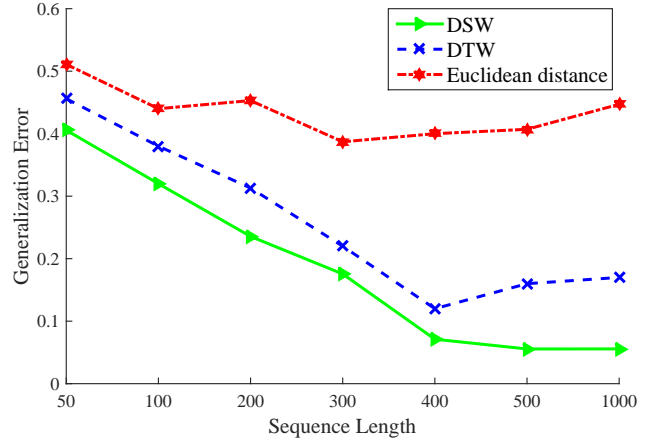


Fig. 11. The generalization trend of three distance measurements facing time series of different length.

order NARMA sequences:

$$s(t+1) = 0.3s(t) + 0.05s(t) \sum_{i=0}^9 s(t-i) + 1.5u(t-9)u(t) + 0.1$$

$$s(t+1) = \tanh(0.3y(t) + 0.05y(t) \sum_{i=0}^{19} y(t-i) + 1.5u(t-19)u(t) + 0.01) + 0.2$$

where $s(t)$ is the output sequence, $u(t)$ is the input sequence, $u(t)$ is independently and identically generated in the range $[0,0.5]$ according to uniform distribution. These two kinds of sequences are generated using the same input sequence. The 10 order and 20 order NARMA sequences are treated as two classes. The original sequences are illustrated in Figure 10.

We use the NARMA model of 10 order and 20 order respectively, to generate synthetic data with varying sequence length. This experiment aims to present what will happen when sequence length is becoming longer and longer. In detail, we generate 10 order and 20 order NARMA sequences of the length in $\{5000, 10000, 20000, 30000, 40000, 50000, 100000\}$. For each length, the generated sequences are then divided into non-overlapping subsequences to obtain 100 subsequences. We randomly select 25 sequences of 10 order and 25 sequences of 20 order as the training set of size 50. The rest 50 subsequences are used as test set. We use 1NN classifier to classify the test set using the training set. For each length, the synthetic dataset is generated 10 times and the classification is also repeated 10 times. The average generalization error rate is collected as the final result.

Figure 11 demonstrates the performance of different distance measurements in terms of varying sequence length. From Figure 11, we can make three main observations: (1) It shows that Euclidean distance scales poorly to long sequences. When the sequence length exceeds 400, Euclidean distance begins to degrade the generalization performance of 1NN classifier. This result is as expected and consistent with our intuition that Euclidean distance is not suitable for long series. (2) The performance of DTW initially improves

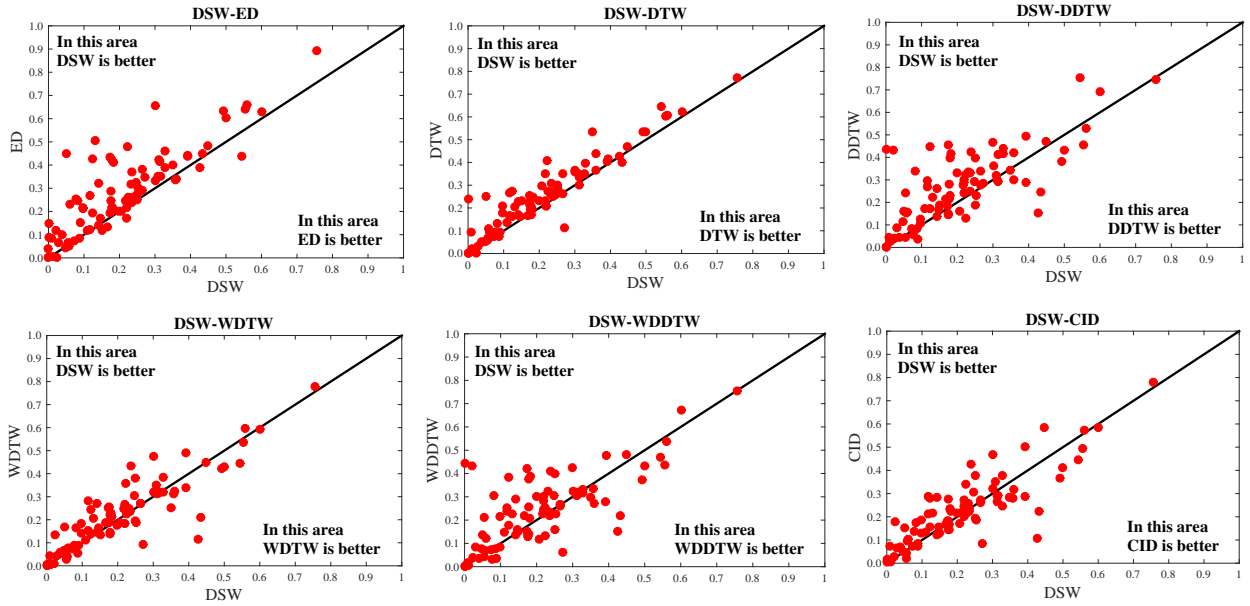


Fig. 12. The pairwise comparison of 1NN classification performance of DSW, ED, DTW, DDTW, WDTW, WDDTW and CID-DTW on 85 UCR time series datasets.

TABLE 1

Number of datasets on which DSW perform better than compared methods using 1NN classifier.

	ED	DTW	DDTW	WDTW	WDDTW	CID
DSW	70	74	62	55	51	51

The numerical value means the number of wins of DSW in comparison with a compared method on 85 datasets. It is observed that DSW is better than compared methods on most datasets. Note that the derivative, weight and complexity penalty are easy to be incorporated in DSW, which may further enhance the performance of DSW.

when facing long sequences. Its performance is much better than Euclidean distance. This result explains why DTW is so successful in sequence processing domains [7], [9]. Sequences are usually long and the time points are usually much larger than the number of observations. However, when sequence length grows longer than 600 points, the performance of DTW begins to worsen. (3) Unlike the competitive distance measurements, DSW is consistently improving the performance in our experiment.

4.4 Classification Performance on Benchmark Datasets

Datasets Our experiments are performed using the UCR time series datasets [18]. The 85 UCR datasets [18] are collected from different domains such as insect recognition, medicine, engineering, motion tracking, image and synthetic data etc. The datasets have already been divided into training and test set. The length of sequences varies from one dataset to another, with the minimum length 24 and maximum length 2709. In each dataset, the sequences are of equal length. The size of datasets varies from 24 to 8926. The number of classes varies from 2 to 60. Detailed information about the datasets is available on the website [18].

Experiment Setup and Parameter settings Our results are averages over 10 repetitions. In each repetition, the

network is optimized by selecting one network from 20 randomly initialized networks using leave-one-out cross validation (LOOCV). The input dimensionality of reservoir network is set as 2. The reservoir size is set as 5. The spectral radius scaling is set as 0.85. This setup is applied to all datasets.

In our experiment, the network is selected in this arbitrary manner. Thus the results may not be optimal for our method. We can of course design specific networks for different datasets by using the result of following subsections 4.6. We do not optimize the classification result using more advanced strategy to simplify operations. However, when dealing with real-world problems, one can of course choose a better parameter setting using simple search strategies e.g. grid search. For example, on BeetleFly dataset, we search the eigenspectral scaling using the range reported in subsection 4.6.1 and improve the accuracy of DSW by 15%. Indeed, our results show that even using randomly generated reservoir and our LOOCV strategy can yield surprisingly good results.

The Euclidean distance and DTW algorithm are determined thus only one run is performed on each dataset.

Compared methods The seven compared method are:

(1) **ED**: Each of the test sequences is compared to the sequences in the training set by Euclidean distance. Then the label of the nearest neighbor of the query is returned as the prediction label.

(2) **DTW**: For each sequence in test set, we compute a distance between this sequence and all training sequences. The distance is computed using DTW. Then we scan all the training set to find a training sequence that is nearest to the given query. The predicted label is taken as the label of the nearest sequence in the training set.

(3) **DDTW**: The first order distance is calculated for DTW as in [12]. Points with similar derivative are more likely to be matched.

(4) **WDTW**: A multiplicative weight penalty is incorpo-

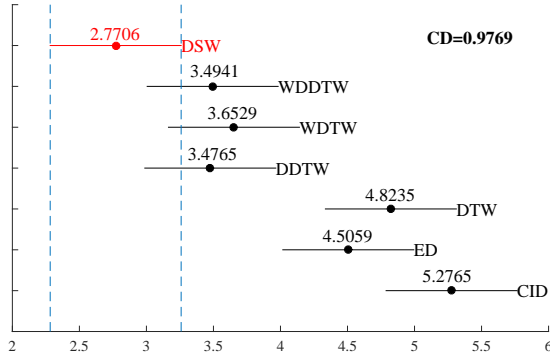


Fig. 13. Critical difference diagram for ED, DTW, WDTW, DDTW, WDDTW, CID-DTW and DSW. The numerical values indicates the average rank on 85 UCR datasets. The difference is significant for algorithms with non-overlapped CDs. DSW performs significantly better than ED and DTW according to the Nemenyi test under the significance level 0.05.

rated to reduce the warping degree. The distance between two points on two series is then $w_{|i-j|}(Q^i - C^j)^2$. Following [19], we employ a logistic function for the weight, i.e., $w_a = \frac{1}{1+g^{(a-L/2)}}$, where $a = 1, 2, \dots, L$, L is the sequence length, g is set on a validation set.

(5) **WDDTW**: A combination of DDTW and WDTW, which considers the derivative and weight penalty simultaneously [19].

(6) **CID-DTW**: As indicated in [10], a complexity penalty is multiplied on the original DTW distance to take into account the difference in the complexity of two series.

(7) **DSW**: The training sequences are converted into state sequences using a reservoir network. When a query sequence arrives, it is first converted into state sequence using the same network. The distance between the query sequence and training sequences is computed by DTW using the state sequences. The network parameters e.g. the connection weights, are initialized randomly.

Platform The experimental environment is Matlab 2015a on an Intel Pentium Quad-Core G2120 3.10GHz CPU with 4GB RAM.

Using the parameter-free 1NN classifier enables us to compare the generalization error rates of DSW with compared algorithms in a pair-wise fashion. The classification result on 85 UCR datasets is presented in Figure 12.

It is clear that our method achieves lower classification error rates than ED and DTW. DSW also performs favorably than more advanced algorithms. In detail, DSW achieves better performance on 70 out of 85 datasets than Euclidean distance. It has better performance on 74 datasets than DTW. The number of datasets on which DSW performs better than compared methods are reported in Table 1.

Statistical Analysis To provide more insights into the performance of our method compared with ED and DTW, etc., we perform statistical significance test for the difference of all approaches. In detail, the generalization error rates of the compared methods on all 85 UCR datasets are first converted into ranks. Then we average the ranks across all datasets. We employ the Friedman test to compare the different distance measurements. The Friedman test indicates that the three distance measurements indeed behave differently. A post-hoc pairwise Nemenyi test is performed

to evaluate the significance of the rank differences. The result is demonstrated in Figure 13. The main observation is that DSW gets the lowest rank and is the best distance measurement of the compared methods for classification. We also observe that our method is significantly better than ED and DTW. In addition, the difference is not significant between Euclidean distance and DTW under the significance level 0.05.

4.5 Texas Sharpshooter Plot

We have evaluated the performance of DSW compared with Euclidean distance and DTW. The result is encouraging. Note that, it would make no sense if we cannot know ahead of time whether DSW will perform well on a given dataset [10]. For this purpose, we employ the Texas sharpshooter plot to visualize if DSW is useful by predicting the generalization ability using the classification results on the training set.

Let us take algorithm A and algorithm B as an example. In detail, we use the LOOCV performance on the training set of algorithms A and B to compute the expected performance gain: training accuracy of A /training accuracy of B ; we use the accuracy on the test set to compute the actual performance gain: test accuracy of A /test accuracy of B . The result for Euclidean distance, DTW and DSW are presented in Figure 14. The true positive (TP) region represents datasets on which we predict a performance gain and are correct. The true negative (TN) region represents datasets on which we predict a performance reduction and are correct. The false negative (FN) region represents datasets on which we predict a performance reduction but it actually turns out to be a performance gain. The false positive (FP) region represents datasets on which we predict a performance gain but actually observe a performance reduction. The FP region is not desired. From Figure 14, we observe that 4.7% points are in the FP region of DSW vs. ED; 8.2% points are in the region of FP for DSW vs. DTW. This result indicates that we have a very low probability to be overoptimistic on our prediction. Besides, note that most points in FP are close to point (1,1), which means the performance reduction is very small.

Up till now, we have compared DSW with Euclidean distance and DTW to demonstrate the effectiveness of our method for sequence classification. Next we will empirically analyze the influence of the relating properties of reservoir model on DSW.

4.6 What is happening in the reservoir?

The skeptical readers may be wondering how a randomly generated reservoir network could achieve excellent classification performance. In this subsection, we are going to empirically uncover some insights about the reservoir network of DSW. In particular, we will analyze the spectral radius scaling of reservoir (4.6.1), the input connection weights (4.6.2), the predictability of reservoir for input sequences (4.6.3), the size of reservoir (4.6.4) and the input dimensionality (4.6.5). Our strategy to evaluate these properties is to fix the other parameters and only vary the target property. The generalization error of DSW is calculated by the 1NN classifier.

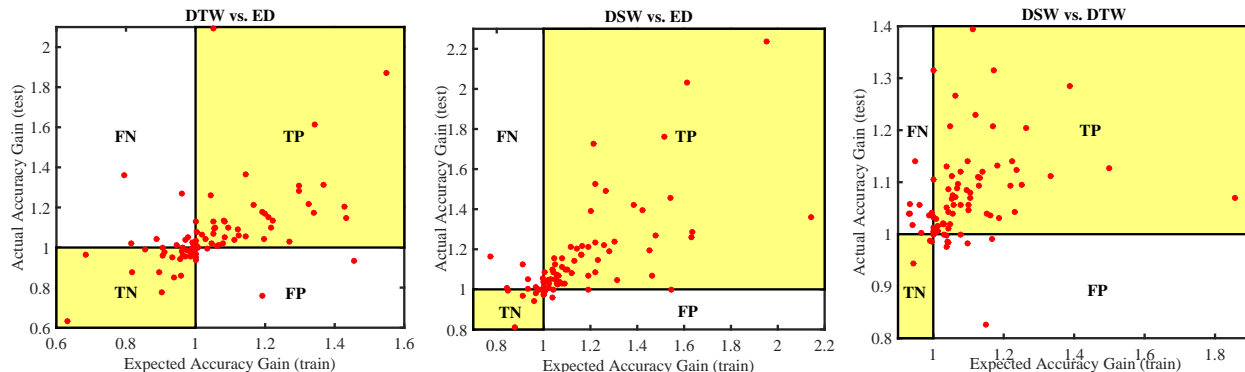


Fig. 14. Texas sharpshooter plot: expected performance gain on the training set vs. actual performance gain on the test set. On most datasets, we can correctly predict the performance of DSW. TP: performance gain on both training and test set; TN: performance reduction on both training and test set; FN: performance reduction on training set but performance gain on test set; FP: performance gain on training set but performance reduction on test set. The FP region means that DSW is overoptimistic about its performance and is not desired. We only observe 4/85 datasets fall into FP region for DSW vs. Euclidean distance and 7/85 datasets fall into FP region for DSW vs. DTW. In FP region, most datasets are close to $[1, 1]$, which indicates the reduction is very small.

4.6.1 Spectral Radius Scaling

Previous studies have revealed that the spectral radius scaling should be less than one to guarantee echo state property [26]. That is sequence modeling should be not sensitive to the initial value of the sequence. In particular, we have $\mathbf{R} = \text{scaling} \times \mathbf{R}/\max(\text{eig}(\mathbf{R}))$, where \mathbf{R} is the reservoir weight matrix [26].

To study the effect of the scaling on the classification performance of DSW, we fix the reservoir parameters and then vary the spectral scaling parameter. In detail, let $r_i = 0.2$, $r_c = 0.5$, $r_j = 0.4$, $N = 5$ and $\text{jumplength} = 2$. The scaling parameter varies from 0.1 to 1.9 with step size 0.2.

We artificially divide some UCR datasets into two groups according to whether the sequences are fast oscillating ones or slowly changing ones. Fast oscillating series changes rapidly over time, while the opposite is slowly changing series that evolve smoothly over time. The separation of the two groups is performed visually since it is difficult to give a definition to separate them. The aim of doing so will be clear later.

Generally, there is a trade-off between the input and the previous state in learning the current state representation. In particular, smaller scaling parameter weights the previous state less and gives more importance to the current input, resulting in short short-term memory [26]. On the opposite, large scaling endows more influence to previous state, which leads to long short-term memory. Oscillating sequences usually need a short short-term memory to model the fast dynamics. Thus small scaling parameter is preferred. Smooth sequences warrant a long short-term memory to take into account far earlier time points. It usually needs a larger scaling parameter.

Figure 15 presents the result of the generalization error rates varying with different scalings. The upside row is for oscillating series and the downside row is for smooth series. It is clear from Figure 15 that severely oscillating sequences usually require a small spectral scaling, while sequences with slow dynamics need a larger scaling. However, Gun-Point dataset and ShapeletSim dataset show contrary result. For example, on Gun-Point dataset, which contains smooth sequences, yet the classification result is optimal when the

scaling is small. ShapeletSim is a dataset which contains oscillating sequences but warrants a large scaling.

Two factors are responsible for the observation on Gun-Point and ShapeletSim datasets:

(1) The first is from the aspect of modeling the sequence dynamics. Generally speaking, on the one hand, to capture the fast dynamics of sequences, the reservoir should put less stress on the far earlier time points and concentrate more on the information of nearby time points. This leads to a need for a short short-term memory ability. On the other hand, to capture the difference between smooth sequences, long short-term memory ability is helpful to capture the global structure information.

(2) The second is the intra-class discriminative features. Since our task at hand is classification, sometimes the discriminative features are more important than dynamics modeling. Depending on the discriminative features are local or global characteristics, a corresponding short-term memory ability and scaling are needed. In particular, small scaling is helpful if the discriminative features spread locally. When the discriminative features are global characteristics, large scaling is preferred.

We examine closely on Gun-Point dataset. Figure 16 explains the observation. The Gun-Point dataset contains two classes that differ from each other by a small region, i.e. taking a gun or no gun, as introduced in Section 1. The reservoir with a small scaling memory nearby points when converting time points into states. Therefore, the discriminative features are discovered. According to Figure 16, for a small scaling parameter, the reservoir provides high dynamics enlarging the minor difference. On the other hand, when the scaling parameter is large, the reservoir representation is more smooth, hiding the small difference between two classes. To make the experiment reproducible, we have fixed the reservoir parameter as above mentioned.

ShapeletSim dataset contains two class of sequences, which oscillate severely. The two classes are generated with two frequencies respectively, which is the main discriminative feature. The within-class sequences differ from each other by a phase shift, which results in their different shapes. To capture the inter-class difference, DSW needs long short-

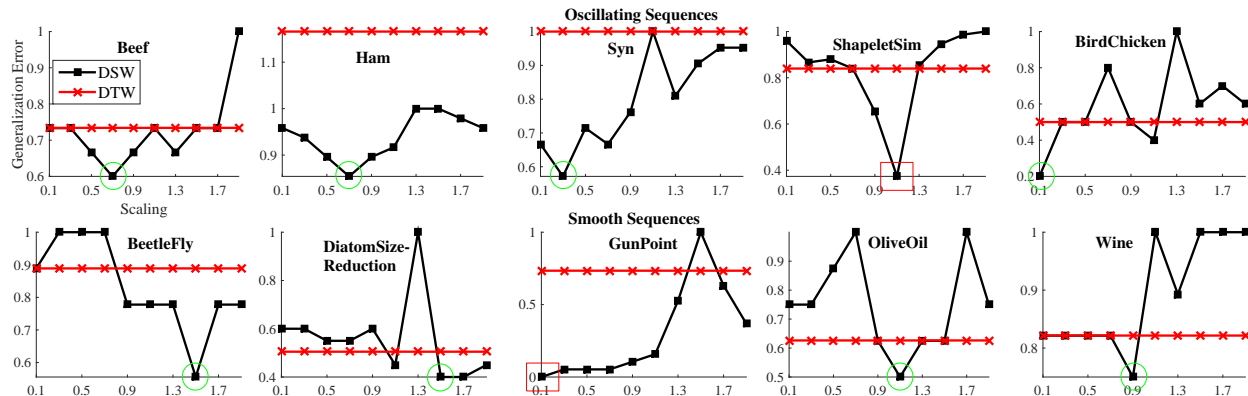


Fig. 15. Generalization error with varying reservoir scalings. The original error rates on each dataset have been divided by the maxima error rate for better visualization. The top row shows the result of fast oscillating sequences and the bottom row shows the result of the smooth sequences. It demonstrates that (1) oscillating sequences usually need a small scaling and smooth sequences usually need a large scaling (see green circle); (2) local discriminative features need small scaling and global discriminative features need large scaling (see red rectangle). In addition, we plot the DTW generalization error for comparison. Note that DSW’s parameters are set arbitrarily without optimizing by cross-validation. Despite the pessimistic setup of DSW, on most dataset DSW maintains lower error than DTW.

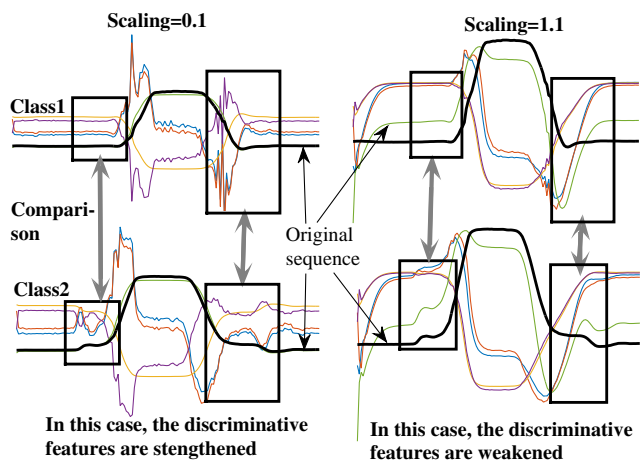


Fig. 16. State sequences (colored) of original sequences (black) in GunPoint dataset. The scaling parameters are 0.1(left) and 1.1(right). The box shows the local discriminative features of two sequences (upside and bottom). Small scaling is good for local discriminative features. Large scaling is good for global discriminative features. Remind that the discriminative features for GunPoint dataset lies in a local area (see the box). The figure demonstrates that small scaling strengthens the discriminative features (left). Yet large scaling makes the discriminative features weaken thus hides them (right).

term memory to distinguish the two frequencies, thus the result (Figure 15) shows it performs best when the scaling is relatively large.

We find two main results in this experiment: (1) Large scaling contributes to long short-term memory and small scaling contributes to short short-term memory. In DSW, this can be a guideline in designing reservoir for modeling sequences. (2) When the discriminative features concentrate on a small region of sequences, small scaling is preferred to strength them; when the discriminative features are global structures, large scaling is useful.

To summarize, for classification, the key concern is to discover the inter-class discriminative features. Normally, despite the specific warrants of some datasets, on most

datasets, it is observed that fast oscillating dynamics benefit from small scaling parameter and more smooth sequences need larger scaling parameter.

4.6.2 Input Weight

The reservoir receives the current input and transforms into a new state by incorporating this input with the previous reservoir state. There is a trade-off between the current input and previous input history.

We fix the reservoir parameters as the same for the previous subsection. The input weight varies from 0.1 to 1.9 step by 0.2. Figure 17 demonstrates the results. It shows small input weights is helpful for long short-term memory and large input weights for short short-term memory. This observation is consistent with the result of spectral scaling.

4.6.3 The Predictability of Reservoir Model

We employ the predictability of readout layer as a proxy for how well the state space representation approximate the original sequences.

The reservoir model is trained to approximate the function mapping from input sequences to output sequences. Define the predictability of a reservoir as the difference between the empirical output and true output. To provide more insights into the reservoir model in DSW, we analyze the relationship between the predictability on training set and classification performance on test set. We train the reservoir model using one-step forward prediction. Ridge regression is employed to learn the output weights [2], [26]. The ridge regression parameter is selected in $\{10^{-5}, 10^{-4}, \dots, 10\}$ by 5-fold cross validation [2]. In detail, we run 10 repetitions for each of the 85 UCR datasets. The reservoir network is regenerated randomly every time. The predictability and generalization error of every network is recorded. We then normalize the two values to have zero mean and unit standard deviation.

By doing so, we can use the predictability of the network on training set as an indication of the classification performance on test set. We examine the relationship between

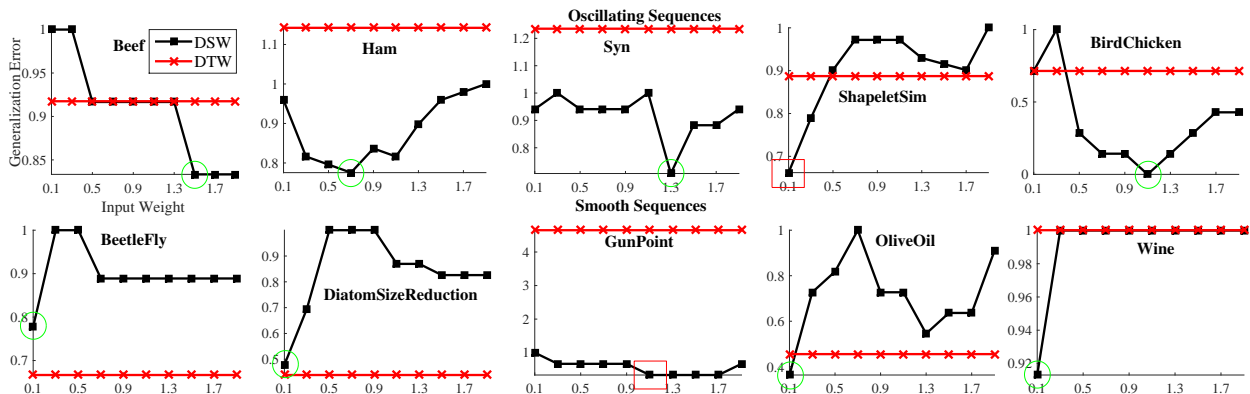


Fig. 17. Generalization error with varying input weights. The original error rates on each dataset have been divided by the maximum error rate for better visualization. The top row shows the result of fast oscillating sequences and the bottom row shows the result of the smooth sequences. It demonstrates that (1) oscillating sequences usually need a large input weight and smooth sequences usually need a small input weight (see green circle); (2) local discriminative features need a small input weight and global discriminative features need a large input weight (see red rectangle). In addition, we plot the DTW generalization error as a comparison. Note that DSW’s parameters are set arbitrarily without optimized by cross-validation. Despite the pessimistic setup of DSW, on most datasets DSW maintains lower error than DTW.

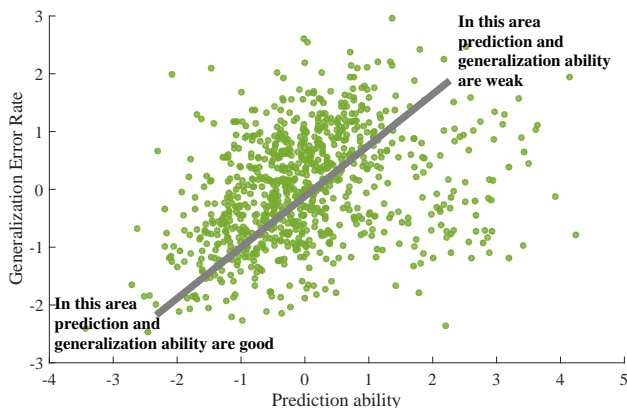


Fig. 18. The correlation between predictability of reservoir network and the generalization error rate of DSW. For visualization, the predictability and generalization error are normalized to have zero mean and unitary standard deviation.

the predictability on the training set and the classification error rate on test set. Figure 18 plots the correlation between these two values on all datasets. The Pearson correlation coefficient is 0.3342, which indicates these two variables are indeed correlated. Therefore, for DSW, it is important to obtain good classification performance by having a reservoir network that can approximate the original data well.

4.6.4 The Size of Dynamic Reservoir

The number of neurons in the reservoir has an influence on the memory capacity of reservoir models [26]. Large reservoir provides more nonlinearity and dynamics. To study how the reservoir size affects DSW, we do experiments on 42 old UCR time series datasets with different reservoir size, ranging in $\{5, 10, 15, 20, 25, 30, 40, 50, 60, 70\}$. We fix the reservoir parameter as $r_i = 0.2$, $r_c = 0.3$, $r_j = 0.4$, $N = 5$ and $jumplength = 2$. On each dataset, we obtain a set of generalization error rates corresponding to different reservoir size. The error rates are then sorted so that each value associates to a rank. The algorithm with the minimum

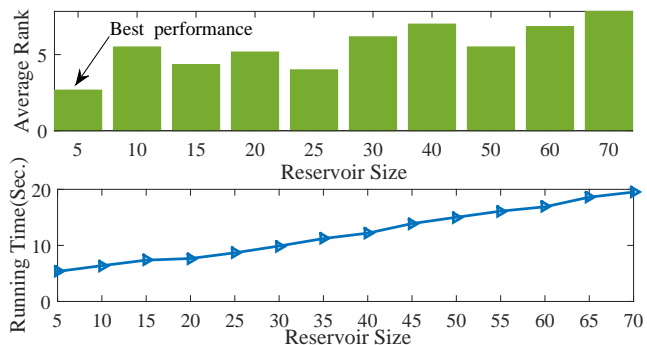


Fig. 19. The average rank on 42 old UCR time series datasets with respect to reservoir size (upside). It demonstrates that small reservoir size is enough to yield good classification results for DSW. And the bottom row presents the running time of DSW w.r.t. reservoir size.

generalization error obtains the rank of 1 and the second minimum gets the rank of 2 etc. The lower rank indicates better performance. We record the average rank of classification performance on each reservoir size.

Figure 19 presents the experimental result. The upside row is the average rank for different reservoir size. Surprisingly, it shows that the reservoir size has very limited influence on the performance of DSW. The rank of the error rate is good when the reservoir size is relatively small. In particular, it performs very well when the reservoir size is 5. It is reasonable to observe this result, since our task is to discriminate the examples in different classes instead of modeling the nonlinear dynamics. The bottom row presents the computational time on Beef dataset for different reservoir size. We observe that with larger reservoir, more computational time is needed. DSW is able to improve the classification performance with tolerable computational cost.

Note that in previous literatures [26], [27], the size of reservoir is usually set as hundreds of neurons to capture the generating mechanism. In our study, we concern different aspects of sequences. The reservoir in our work is

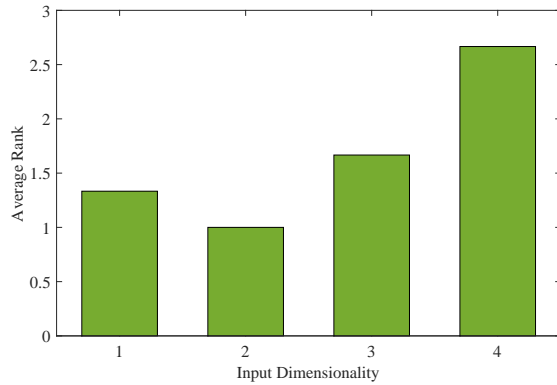


Fig. 20. The average rank of generalization error for different input dimensionality.

mainly to provide versatile discriminative features to help classification. As a result, we do not need too large reservoir size.

4.6.5 Input Dimensionality

The dimensionality of input influences the resulting state sequences. For n input dimensionality, it means we feed n successive time points as the input into the reservoir to obtain an updated state. We extend the original sequence by repeating the end of sequences n times so that the state sequences are of the same length as the original sequences.

We perform experiments on 42 old UCR datasets using different input dimensionality. On each dataset, the input dimensionality is selected as 1,2,3 and 4. Then using the selected input dimensionality, we learn reservoir state sequences. We have fixed the reservoir parameters during the experiment to guarantee only the input dimensionality is varied. The parameters are the same as that of subsection 4.6.1. Figure 20 illustrates the average rank of each dimensionality over all 42 datasets. It clearly demonstrates that 2 input dimensionality achieves the best performance, followed by 1 dimensionality. However, for 3 and 4 dimensionality it performs much poorer.

5 CONCLUSION

In this paper, we propose a novel algorithm, DSW, for calculating the distance between sequences. DSW employs a reservoir network as a general purpose nonlinear temporal filter. The original sequences are first converted into reservoir state trajectory sequences to capture the autocorrelation structure information. The state trajectory sequence provides versatile discriminative features for classification. Then dynamic programming is performed to find an alignment between two state sequences. Therefore, points with similar states are matched. The time complexity of DSW is at the same level as that of DTW ($O(L_Q L_C)$).

We have conducted extensive experiments to evaluate DSW using both synthetic datasets and benchmark datasets, compared with DTW and its variants. The experimental results demonstrate the competitiveness of DSW. In particular, DSW achieves state-of-the-art classification performance on 85 UCR time series data. DSW is also empirically demonstrated to be endowed with better robustness and scalability.

Possible extensions of this work include: (1) to provide more efficient optimization methods for the reservoir network in DSW. (2) to design accelerating techniques for searching alignments in DSW.

REFERENCES

- [1] Y. Jo, N. Loghmanpour, and C. P. Rosé, "Time series analysis of nursing notes for mortality prediction via a state transition topic model," in *Proceedings of the 24th ACM International on Conference on Information and Knowledge Management*, pp. 1171–1180, ACM, 2015.
- [2] H. Chen, P. Tino, A. Rodan, and X. Yao, "Learning in the model space for cognitive fault diagnosis," *IEEE Transactions on Neural Networks and Learning Systems*, vol. 25, no. 1, pp. 124–136, 2014.
- [3] R. Goroshin, J. Bruna, J. Tompson, D. Eigen, and Y. LeCun, "Unsupervised learning of spatiotemporally coherent metrics," in *Proceedings of the IEEE International Conference on Computer Vision*, pp. 4086–4093, 2015.
- [4] W. Pei, D. M. Tax, and L. van der Maaten, "Modeling time series similarity with siamese recurrent networks," *arXiv preprint arXiv:1603.04713*, 2016.
- [5] H. Chen, F. Tang, P. Tino, and X. Yao, "Model-based kernel for efficient time series analysis," in *Proceedings of the 19th ACM SIGKDD international conference on Knowledge discovery and data mining*, pp. 392–400, ACM, 2013.
- [6] H. Chen, F. Tang, P. Tino, A. G. Cohn, and X. Yao, "Model metric co-learning for time series classification," in *Proceedings of the Twenty-Fourth International Joint Conference on Artificial Intelligence*, pp. 3387–3394, AAAI Press, 2015.
- [7] A. Bagnall, A. Bostrom, J. Large, and J. Lines, "The great time series classification bake off: An experimental evaluation of recently proposed algorithms. extended version," *arXiv preprint arXiv:1602.01711*, 2016.
- [8] L. Ye and E. Keogh, "Time series shapelets: a new primitive for data mining," in *Proceedings of the 15th ACM SIGKDD international conference on Knowledge discovery and data mining*, pp. 947–956, ACM, 2009.
- [9] T. Rakthanmanon, B. Campana, A. Mueen, G. Batista, B. Westover, Q. Zhu, J. Zakaria, and E. Keogh, "Searching and mining trillions of time series subsequences under dynamic time warping," in *Proceedings of the 18th ACM SIGKDD international conference on Knowledge discovery and data mining*, pp. 262–270, ACM, 2012.
- [10] G. E. Batista, E. J. Keogh, O. M. Tataw, and V. M. de Souza, "Cid: an efficient complexity-invariant distance for time series," *Data Mining and Knowledge Discovery*, vol. 28, no. 3, pp. 634–669, 2014.
- [11] D. J. Berndt and J. Clifford, "Using dynamic time warping to find patterns in time series.," in *AAAI workshop on KDD*, vol. 10, pp. 359–370, Seattle, WA, 1994.
- [12] E. J. Keogh and M. J. Pazzani, "Derivative dynamic time warping," in *SDM*, vol. 1, pp. 5–7, SIAM, 2001.
- [13] F. Zhou and F. De la Torre, "Generalized canonical time warping," *IEEE Transactions on Pattern Analysis and Machine Intelligence*, vol. 38, no. 2, pp. 279–294, 2016.
- [14] J. A. Kogan and D. Margoliash, "Automated recognition of bird song elements from continuous recordings using dynamic time warping and hidden markov models: A comparative study," *The Journal of the Acoustical Society of America*, vol. 103, no. 4, pp. 2185–2196, 1998.
- [15] H. Ding, G. Trajcevski, P. Scheuermann, X. Wang, and E. Keogh, "Querying and mining of time series data: experimental comparison of representations and distance measures," *Proceedings of the VLDB Endowment*, vol. 1, no. 2, pp. 1542–1552, 2008.
- [16] N. Begum, L. Ulanova, J. Wang, and E. Keogh, "Accelerating dynamic time warping clustering with a novel admissible pruning strategy," in *Proceedings of the 21th ACM SIGKDD International Conference on Knowledge Discovery and Data Mining*, pp. 49–58, ACM, 2015.
- [17] L. Ye and E. Keogh, "Time series shapelets: a novel technique that allows accurate, interpretable and fast classification," *Data mining and knowledge discovery*, vol. 22, no. 1-2, pp. 149–182, 2011.
- [18] Y. Chen, E. Keogh, B. Hu, N. Begum, A. Bagnall, A. Mueen, and G. Batista, "The ucr time series classification archive," July 2015. www.cs.ucr.edu/~eamonn/time_series_data/.

- [19] Y.-S. Jeong, M. K. Jeong, and O. A. Omitaomu, "Weighted dynamic time warping for time series classification," *Pattern Recognition*, vol. 44, no. 9, pp. 2231–2240, 2011.
- [20] C. Faloutsos, M. Ranganathan, and Y. Manolopoulos, "Fast sub-sequence matching in time-series databases," in *ACM SIGMOD Record*, pp. 419–429, ACM, 1994.
- [21] D. Garreau, R. Lajugie, S. Arlot, and F. Bach, "Metric learning for temporal sequence alignment," in *Advances in Neural Information Processing Systems*, pp. 1817–1825, 2014.
- [22] F. Petitjean, G. Forestier, G. I. Webb, A. E. Nicholson, Y. Chen, and E. Keogh, "Dynamic time warping averaging of time series allows faster and more accurate classification," in *2014 IEEE International Conference on Data Mining*, pp. 470–479, IEEE, 2014.
- [23] S. S. Haykin, S. S. Haykin, S. S. Haykin, and S. S. Haykin, *Neural networks and learning machines*, vol. 3. Pearson Upper Saddle River, NJ, USA:, 2009.
- [24] T. Mikolov, I. Sutskever, K. Chen, G. S. Corrado, and J. Dean, "Distributed representations of words and phrases and their compositionality," in *Advances in Neural Information Processing Systems*, pp. 3111–3119, 2013.
- [25] L. Maaten, "Learning discriminative fisher kernels," in *Proceedings of the 28th International Conference on Machine Learning*, pp. 217–224, 2011.
- [26] M. Lukoševičius and H. Jaeger, "Reservoir computing approaches to recurrent neural network training," *Computer Science Review*, vol. 3, no. 3, pp. 127–149, 2009.
- [27] A. Rodan and P. Tiño, "Simple deterministically constructed cycle reservoirs with regular jumps," *Neural computation*, vol. 24, no. 7, pp. 1822–1852, 2012.